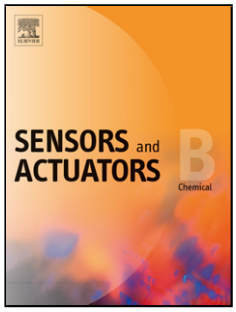

A biomimetic photonic crystal sensor for label-free detection of urinary venous thromboembolism biomarker

Sara Resende (Investigation) (Methodology) (Validation) (Visualization) (Formal analysis) (Data curation) (Writing - original draft), Manuela F. Frasco (Conceptualization) (Funding acquisition) (Supervision) (Project administration) (Writing - review and editing), M. Goreti F. Sales (Supervision) (Funding acquisition) (Writing - review and editing)

PII: S0925-4005(20)30295-1

DOI: https://doi.org/10.1016/j.snb.2020.127947

Reference: SNB 127947

To appear in: *Sensors and Actuators: B. Chemical*

Received Date: 30 October 2019

Revised Date: 2 March 2020

Accepted Date: 3 March 2020

Please cite this article as: Resende S, Frasco MF, Sales MGF, A biomimetic photonic crystal sensor for label-free detection of urinary venous thromboembolism biomarker, *Sensors and Actuators: B. Chemical* (2020), doi: https://doi.org/10.1016/j.snb.2020.127947

A biomimetic photonic crystal sensor for label-free detection of urinary venous thromboembolism biomarker

Sara Resende, Manuela F. Frasco* and M. Goreti F. Sales*

BioMark sensor research/UC, Faculty of Sciences and Technology, Coimbra University, Coimbra, Portugal

BioMark sensor research/ISEP, School of Engineering, Polytechnic Institute, Porto, Portugal

CEB, Centre of Biological Engineering, Minho University, Braga, Portugal

*To whom correspondence should be addressed. E-mail: (MFF) mffrasco@gmail.com; (MGFS) goreti.sales@eq.uc.pt or goreti.sales@gmail.com.

Graphical abstract

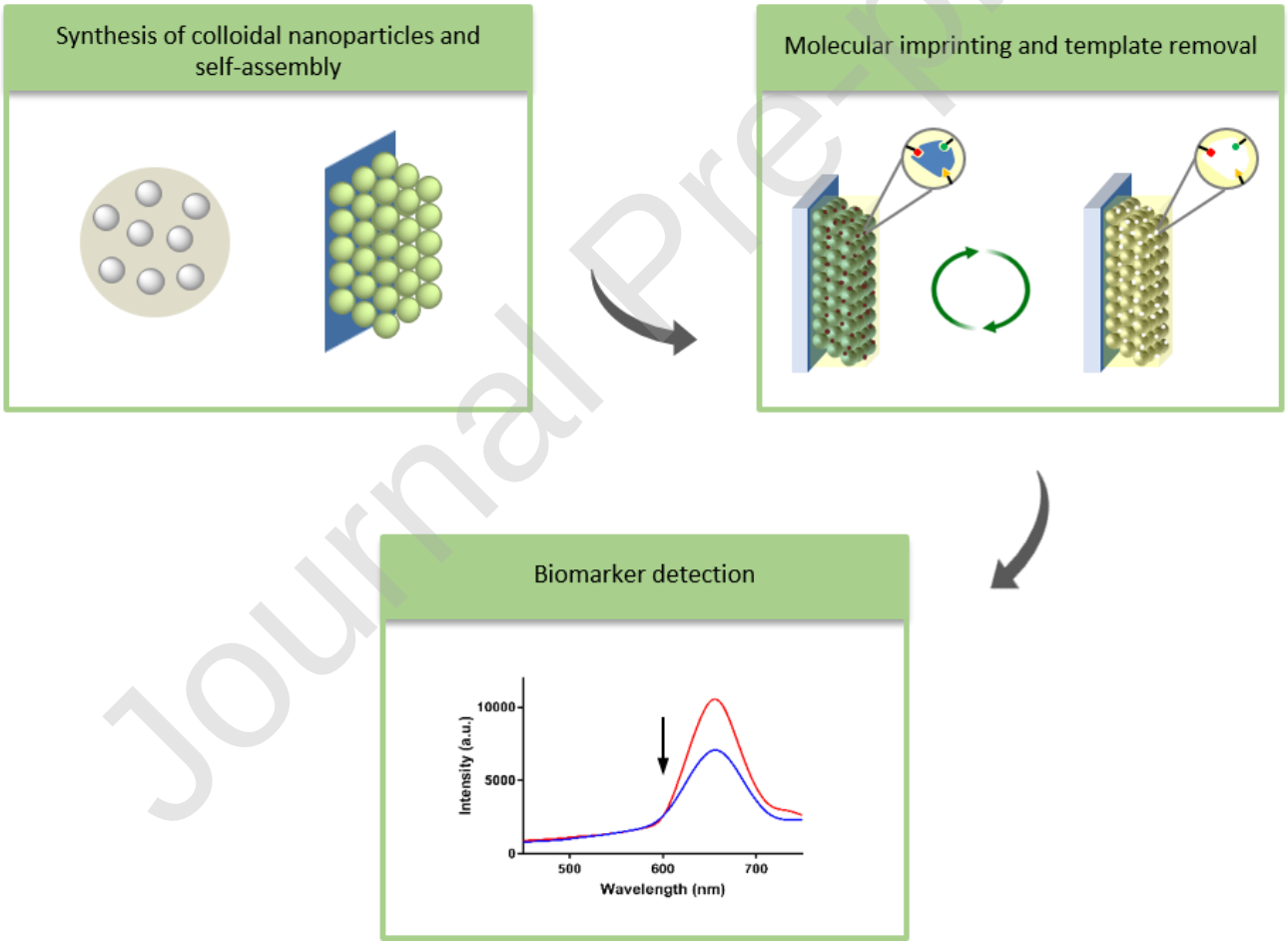

Highlights

- Combining Molecularly-imprinted polymer (MIP) with silica-based photonic crystals
- Highly ordered silica nanoparticles assembled by vertical deposition
- MIP produced on top of organized the ordered silica nanoparticles for fibrinopeptide B (FPB)
- FPB rebinding yielded a reflectance change that was concentration dependent
- Successful application of this approach in human samples

Abstract

This work reports a novel label-free sensor combining photonic crystals and molecularly-imprinted polymer materials for targeting a protein in human samples within levels of clinical interest. This concept was applied to detect fibrinopeptide B (FPB) in urine, a biomarker of venous thromboembolism, which is a disease of great concern and demands innovative point-of-care devices for improved diagnosis.

The molecularly-imprinted photonic polymer (MIPP) was obtained by tailoring an imprinted polymer on highly ordered silica nanoparticles assembled by vertical deposition. Owing to the hierarchical structure, the resulting MIPP exhibited optical properties that changed upon rebinding of the target analyte, FPB. Thus, the changes in reflectance intensity enabled a rapid and sensitive detection of FPB in human urine. The observed response was linear between 0.2 ng mL^{-1} and 22 ng mL^{-1} and showed a limit of detection of 0.13 ng mL^{-1}. These features of the sensing material allow the assessment of urinary FPB at relevant clinical levels. In addition, the sensor was selective for FPB compared to the standard biomarker of venous thromboembolism, D-Dimer. The stability of the material was evidenced by the reusability study, which demonstrated reversibility of the maximum intensity after three cycles of recognition and regeneration. Moreover, the sensor showed good performance for the spiked FPB detection in control human urine.

Overall, the application of such label-free sensor offers high selectivity and stability, as well as easy operation. It may constitute an alternative method for non-invasive and real-time detection of various protein biomarkers in point-of-care.

Keywords: photonic sensor; photonic crystal; molecularly-imprinted polymer; fibrinopeptide B; venous thromboembolism biomarker.

1. Introduction

Venous thromboembolism (VTE) is a pathology in which a blood clot is formed most often in the deep veins of the leg or arm (commonly known as deep vein thrombosis) and travels in the circulation, lodging in the lungs (pulmonary embolism). It is a very common disorder that can occur in all races, ethnicities, age groups and both genders [1]. However, there are some risk-factors like advanced age, immobility, obesity and cancer related-surgery. Moreover, VTE might also be partially heritable [2, 3].

VTE is a major health problem among cancer patients, since cancer itself increases coagulation. Cancer patients have 4 times higher risk (comparing with the general population) of developing blood clots [3, 4]. VTE can occur without any warning signs or symptoms and can go unrecognized and undiagnosed by a healthcare professional. Accurate diagnosis minimizes the risk of thromboembolic complications and averts the exposure of patients without thrombosis to the risks of anticoagulant therapy, hence reducing the total treatment costs [5, 6].

Nowadays, the diagnosis of VTE is performed by monitoring the biomarker D-dimer (a product of fibrin degradation) and ultrasound or computed tomography-imaging techniques [7, 8]. However, there is still debate on which VTE marker is best suited to help diagnose an episode, considering also that comorbidities in high risk patients like in cancer patients may reduce the sensitivity and specificity of a biochemical test [7]. Therefore, it is highly relevant to develop simple sensing technologies that can aid the diagnostic of suspected VTE. Another biomarker involved in the

coagulation cascade and that can be assessed is fibrinopeptide B (FPB) [9]. To the best of our knowledge, FPB levels are currently measured using immunoassays [10]. These methods are time consuming and complex, often requiring the help of professional technicians and the use of expensive equipment, thus contributing for not using FPB assays routinely in diagnostic or treatment monitoring. Therefore, the development of a label-free, simple, fast and low-cost detection method is necessary. Biosensors yield all these features and can answer the demand for more accurate and personalized portable devices [11]. Also, to the best of our knowledge, there is currently no sensor or biosensor device described to this end. In this context, developing a test that could be used as screening tool for VTE based on urine levels of a biomarker such as FPB, which reflects blood clot formation, has great potential.

Recently, the use of low-cost colloidal self-assembly to produce 3D photonic crystals (PCs) for the development of sensors has drawn considerable interest from researchers [12, 13]. PC structures are made of periodic arranged materials with different dielectric constants, exhibiting a photonic band gap whereby forbidding certain wavelengths of light to propagate through the structure. PCs can thus be configured to have distinct wavelengths of reflection and structural colours that can be tuned to change in response to the presence of analytes [14]. Thus, a PC structure enables a label-free transduction that may be easily coupled to biorecognition elements aiming to provide real-time specific detection of target molecules.

Among several biorecognition elements, molecularly-imprinted polymers (MIPs) are attractive materials. They have specific recognition sites that are complementary in shape and size to the target biomarker, created upon a specific polymerization procedure around a template. After removal of the imprinted molecules, the obtained nanocavities exhibit high selectivity for biorecognition. In a context of biomimicry, they offer many advantages such as physical robustness, thermal stability, low-cost and easy preparation. The combination of PCs and MIPs, also known as Molecularly-Imprinted Photonic Polymers (MIPPs), constitutes a feasible alternative to build an optical sensor

and the idea has been studied by several research groups [15]. These sensors allow a direct detection of the analyte via a change of polymer conformation upon target molecule recognition. When the polymer is structured on a PC, the detection of the analyte is enabled by an optical variation of the sensor [16].

MIPPs have been reported for the detection of several molecules, including testosterone [17], cinchonine [18], chloramphenicol [19], tryptophan [20], morphine [21], nitrophenol [22], vanillin [23], bisphenol A [24], atrazine [25], among others. Considering the sensing of biomacromolecules, studies combining protein imprinting and PCs focused mainly on the proof-of-concept of sensor development targeting bovine serum albumin [26] and bovine haemoglobin [27, 28]. These reports showed various surface imprinting approaches on colloidal crystal templates, assembled in films or suspension arrays, and demonstrated good selective affinity and sensitivity. Nonetheless, a thorough literature review yielded no studies on MIPPs analysing disease protein biomarkers in biological matrices.

Thus, the present work describes a novel sensor for FPB based on the merged technology of PCs and MIPs. A highly ordered colloidal array of monodispersed silica nanoparticles was used as support to construct the MIPP. The hierarchical structure was used as mould to assemble the sensing layer with specific binding cavities, i.e., to cast the plastic recognition elements. The MIPP contains the molecular imprints of FPB and exhibits optical properties that change upon detection of low concentrations of the target biomarker in urine.

2. Material and methods

2.1. Reagents

All chemicals were of analytical grade and used without further purification. Tetraethyl orthosilicate (TEOS) and calcium chloride dihydrate were purchased from Merck; ammonium hydroxide 25%, DL-lactic acid and creatinine were obtained from Fluka; *N*,*N*,*N'*,*N'*-tetramethylethylenediamine (TEMED), *N*,*N*-methylenebis(acrylamide) (Bis-A), ethanol absolute, methacrylic acid (MAA), fibrinopeptide B (FPB; molecular weight 1552.56 g mol^{-1}), D-dimer, citric acid and sulphuric acid were purchased from Sigma-Aldrich. Sodium hydrogen carbonate, sodium chloride, magnesium sulphate 7-hydrate, potassium dihydrogen phosphate, hydrochloric acid and ammonium chloride were acquired from Panreac. Urea was purchased from Fagron and dipotassium hydrogen phosphate was purchased from Riedel-de Häen. Glucose was obtained from Fisher BioReagent. Ammonium peroxodisulfate (APS) and nitric acid were obtained from Analar Normapur, acetone from Labsolve and 2-(*N*-morpholino)ethanesulfonic acid (MES) buffer from AppliChem. Ultrapure Milli-Q laboratory grade water (conductivity <0.1 µS/cm) was employed throughout.

The preparation of synthetic urine used the following composition: 1.1 mmol L^{-1} DL-lactic acid, 2.0 mmol L^{-1} citric acid, 25 mmol L^{-1} sodium bicarbonate, 90 mmol L^{-1} sodium chloride, 2.0 mmol L^{-1} magnesium sulfate, 10 mmol L^{-1} sodium sulfate, 7.0 mmol L^{-1} potassium dihydrogen phosphate, 7.0 mmol L^{-1} dipotassium hydrogen phosphate, 25 mmol L^{-1} ammonium chloride, 170 mmol L^{-1} urea and 7.0 mmol L^{-1} creatinine, all mixed in ultrapure Milli-Q water [29]. The pH of the solution was adjusted to 6.0 by addition of 1.0 mol L^{-1} hydrochloric acid.

2.2. Preparation of silica nanoparticles and 3D-ordered silica structure

Highly monodisperse silica nanospheres were synthesized using the Stöber method [30] with some modifications. Briefly, two solutions were first prepared: Solution A was obtained by thoroughly mixing 1.8 mol L^{-1} ammonia, 3 mol L^{-1} ethanol, and 14 mol L^{-1} ultrapure Milli-Q water. Solution B was obtained by mixing 0.2 mol L^{-1} TEOS and 7.8 mol L^{-1} ethanol. Solution B was

quickly added to solution A, under vigorous stirring, which was slowed down after 2 min to a gentle stir for 2 h at 25 ºC. The obtained colloidal suspension was cleaned by several rounds of centrifugation (7000 rpm, 15 min), and the silica nanospheres were dispersed in absolute ethanol.

The 3D ordered silica arrays were prepared via the vertical deposition method. To this end, the obtained silica nanospheres fully dispersed in absolute ethanol at approximately 12 mg mL^{-1} were placed into 5 mL vials. Glass slides (obtained from Deltalab), previously washed sequentially with nitric acid, ethanol, acetone and ultrapure Milli-Q water, were introduced in the solution of nanospheres. The close-packed periodic arrays were obtained when ethanol evaporated.

2.3. Construction of the molecularly-imprinted photonic polymer

The MIPP films were fabricated by imprinting a polymeric network on an opal photonic structure (Figure 1). The nanocavities of the structure made by self-assembly of silica nanoparticles were filled with a polymerization mixture. The solution was prepared with 10 µg of FPB, the functional monomer MAA (25 µL) and cross-linker Bis-A (25 µL) dissolved in 1 mL of MES buffer (0.1 mol L^{-1}, pH 6) and pre-incubated for 30 min at 4 ºC. This pre-polymer solution was added to the colloidal crystal and a second clean glass slide was placed on top, followed by 30 min incubation. The radical polymerization was initiated by adding APS and TEMED. The two slides were firmly held together forming a "sandwich"-type structure to force the liquid to fill the voids within the colloidal crystal structure. After 6h, the MIPP was exhaustively rinsed with ultrapure water and dried with nitrogen. The 6h period was selected after optimization ranging 2 to 12h. The FPB templates were removed using a solution of sulphuric acid 0.5 mol L^{-1} through incubation for 30 min. Before the calibration experiments, the washed MIPP was equilibrated for 30 min in MES buffer (0.1 mol L^{-1}, pH 6). As control, a non-imprinted photonic polymer (NIPP) was prepared in the same way, but without FPB.

PLEASE INSERT FIGURE 1 HERE

2.4. Characterization and optical measurements

The size and morphology of silica nanoparticles and the photonic films were investigated by Scanning Electron Microscopy (SEM), on FEI Quanta 400FEG ESEM/EDAX PEGASUS X4M equipment.

The optical set up comprised a reflection fibre probe (fibre diameter of 200 µm, Dropsens), and a deuterium-halogen light source along with a spectrophotometer (wavelength range of 200 to 1100 nm, Methrom, AG). A diffuse reflectance standard was used as a reference surface and the reflectance at normal incidence was collected using the optical fibre probe.

2.5. Sensing ability of the MIPP towards FPB

The sensing properties of the MIPP were first evaluated using increasing concentrations of FPB (0.2 to 240 ng mL^{-1}) in MES buffer (0.1 mol L^{-1}, pH 6). In a typical experiment, the MIPP was first stabilized in MES buffer. Afterwards, successive concentrations of FPB were incubated for 20 min and the reflectance spectra were collected. In order to determinate the binding affinity of FPB to the PC in the absence of polymer, three successive concentrations of FPB (0.2, 6.0 and 240 ng mL^{-1}) were assayed. After stabilizing the PC in MES buffer, in a similar procedure as it was done for MIPP, the three different FBP solutions were incubated for 20 min each. The sensor ability to detect FPB was also evaluated primarily in synthetic urine, a first approach to analyse the biomarker in a more complex matrix, and furthermore in real human urine samples from healthy individual (after informed consent). The studies in urine were performed after 50-fold sample dilution in ultrapure Milli-Q water to a final FPB concentration range of 0.2 to 22 ng mL^{-1}. Sensor responses were analysed by $И_0$, where I corresponds to the maximum intensity of the peak and I_0 represents the maximum peak intensity of the control spectrum (FPB = 0 ng mL^{-1}). Calibration plots of optical signal ($И_0$) against the logarithm concentration of FPB were evaluated with regard to the linear regression obtained. Following IUPAC procedure for logarithm dependent calibrations [31], the limit

of detection (LOD) was calculated as the concentration taken at the point of intersection of the linear range and a line parallel to the x-axis through the mean intensity value measured in the lowest concentration. For the selectivity studies, human urine samples, also diluted 50-fold, were spiked with FPB and/or D-dimer at final concentrations of 1 ng mL^{-1} and 7 ng mL^{-1}, separately or combined. Sensor reusability was analysed by reflectance intensity after cycles of incubation for 20 min with 22 ng mL^{-1} FPB in human urine followed by removal with sulphuric acid and equilibration in MES buffer, similarly to the calibration studies. To evaluate the practical applicability of the MIPP response, human urine samples were spiked with FPB at known concentrations of 30, 100 and 350 ng mL^{-1}, diluted 50-fold for fitting in the linear regression obtained from the calibration curves. All experiments were performed at room temperature and all conditions were also tested on NIPP as control.

3. Results and Discussion

3.1. Characterization of the opal film

In order to prepare the close-packed array with a visible structural colour, silica nanoparticles of various sizes were first synthesized by adjusting the reaction parameters, such as amount of TEOS and temperature [32, 33]. The silica colloidal crystal arrays were prepared by vertical deposition on glass substrates, forming a highly ordered 3D structure, later used as template for the subsequent formation of the imprinted polymer.

The best opal film obtained had spherical silica particles with an average size of 270 ± 10 nm. It showed a light red colour (Figure 2A) that reflected in the visible light region around 600 nm (Figure 2B). The periodic structure of the opal film was evident in SEM images as well as the monodispersity of silica nanoparticles (Figure 2C), which favoured the self-assembly and the production of a close-packed crystal structure (Figure 2D). A better monodispersity leads to a larger

uniform area and less cracks. Some cracks were however visible, due to the fast evaporation of ethanol during the self-assembly [34]. Nonetheless, it presents unique optical properties, herein useful for sensor development.

PLEASE INSERT FIGURE 2 HERE

3.2. Optical response of the MIPP

It is expected that the periodicity and/or refractive index of the FPB imprinted matrix changes with the amount of the target analyte, for which the reflectance of the MIPP sensors against different concentrations of FPB shall also change. This variation is useful for quantitative purposes.

The polymeric sensing materials on the opal film were obtained by polymerizing monomer, cross-linker and template (MIPP, Figure 1), and yielded a significant decrease in the reflectance value, which recovered after template removal with an acidic solution (Figure S1A). In contrast, the polymerization with only monomer and cross-linker (NIPP) yielded little changes in the reflectance data (Figure S1B). As another control experiment, it was also evaluated if FPB would have any affinity to bind silica NPs composing the PC in the absence of the polymer matrix. Results in Figure S2 revealed that, in the absence of polymer, the peak intensity of the PC does not change significantly upon incubation with FPB. Thus, these results suggest that the reflectance values of the photonic sensor changed almost exclusively with FPB in the presence of an imprinted polymer network.

Furthermore, to investigate the optical quantitative properties of the sensor, both MIPP and NIPP sensing surfaces were incubated with increasing concentrations of FPB to trace calibration curves for the sensing material and the corresponding control. Different conditions were tested to this end by preparing FPB solutions in MES buffer and diluted synthetic and human urine.

As expected, consecutive additions of FPB solutions in MES buffer changed the optical properties. Small shifts of the Bragg diffraction peak were observed but a significant decrease of the

intensity of MIPP reflectance was evidenced in a concentration dependent way (Figure 3A). In contrast, NIPP control material yielded a random response (Figure 3B). These results suggest that the response obtained by the imprinted film was dominated by the specific recognition cavities tailored for FPB within the interstices of the opal structure. As the empty imprinted sites were being occupied by the target molecule, there was a reduction in peak intensity. The observed decrease may be attributed to different factors like an alteration of the refractive index in the presence of FPB, as reported by previous studies [34-37]. In terms of analytical features, the MIPP calibration in buffer displayed a linear behaviour between 0.2 and 240 ng mL^{-1} with a slope of -0.171 (R^2 = 0.986), quite different from the random NIPP response (Figure 3C).

Preceding the analysis in human urine, the behaviour of the sensing material was evaluated in synthetic urine samples. As observed in buffer, the MIPP material evidenced a decreasing trend of the reflectance intensity upon binding of FPB, while the NIPP material had a random response (Figure S3). The linear trend observed for the MIPP calibration was within the range 0.2 until 22 ng mL^{-1}, with a slope of the linear trend of -0.236 (R^2 = 0.998), corresponding to an LOD of 0.12 ng mL^{-1}. The slope of the linear trend increased in comparison to buffer, which is a good feature in terms of analytical application. To understand if this behaviour would be the same in real human urine, a similar calibration was performed. A MIPP linear response with a slope of -0.295 (R^2 = 0.994) and a similar LOD of 0.13 ng mL^{-1} was obtained (Figure 3D), while the NIPP maintained its random response (Figure 3E). The analysis of real samples correlated well with the calibration in synthetic urine and their better slope in comparison to buffer suggests that this could be an effect of the ionic content in urine thereby reflecting the presence of given compounds. The calibrations obtained for all matrices are also compared in Figure S4.

Since the experiments in both synthetic and real urine were performed with a 50-fold diluted sample matrix, this means that the concentrations tested in real sample analysis should cover the range of values observed in healthy people and VTE patients. Indeed, the presence of 6.5 ng mL^{-1} (a

concentration 50-fold higher than LOD) can be detected in a real urine sample. According to previous studies, a VTE positive patient (ill) would have a concentration of approximately 80.0 ng mL^{-1}, while a negative patient would have maximum 10.0 ng mL^{-1} [10]. Therefore, the developed MIPP sensor can be applied in the onset of the disease, non-invasively, being able to distinguish healthy from diseased conditions.

PLEASE INSERT FIGURE 3 HERE

3.3. Selectivity of FPB detection in human urine

The selectivity of MIPP for FPB detection in human urine was examined against D-dimer (DD), considered a highly sensitive biomarker of VTE, as interfering peptide. The concentration of DD found in the urine of VTE positive patients is around 150 ng mL^{-1} [38]. The concentrations of both biomarkers upon testing the possible interference of DD in FPB selective detection were chosen according to the levels found in urine of healthy and diseased people, respectively [10, 39]. Accordingly, the final concentrations of 1.0 ng mL^{-1} and 7.0 ng mL^{-1}, in 50-fold diluted samples, mean that the real accessed values would be 50 ng mL^{-1} and 350 ng mL^{-1}, respectively.

In general, there were clear differences between the MIPP sensor response to FPB or the interfering species DD (Figure 4). When incubated with DD at 1.0 ng mL^{-1} and 7.0 ng mL^{-1}, the signal in respect to the blank solution was 96.4 ± 1.8% and 108.7 ± 13.2%, respectively. As the maximum intensity of peaks had no significant difference, these results confirmed the null effect of the DD in terms of the analytical response of the sensor. Moreover, the sensor was incubated with mixed solutions of DD and FPB, also at concentrations of 1.0 ng mL^{-1} and 7.0 ng mL^{-1}, and the signal generated was 62.9 ± 3.6% and 38.8 ± 4.3%, respectively. These values compared well with those produced by the single standard solutions of FPB (Figure 4C), thereby confirming that DD did not interfere on the MIPP response to FPB and supporting the good selectivity of this sensor.

The NIPP was tested under the same conditions and no significant optical change was observed (Figure 4C). Overall, the response of NIPP sensor to FPB at 1.0 ng mL^{-1} and 7.0 ng mL^{-1} corresponded to 102.8% ± 7.5%, and 99.2% ± 7.6%, of the blank signal, respectively. The corresponding relative reflectance of the DD single solution was 91.2% ± 5.5%, and 96.9% ± 17.8%. When testing mixtures of FPB with DD, similar values of 98.5 ± 14.3% and 97.4 ± 7.2% were obtained, showing a slightly higher average. It is also important to highlight that the relative standard deviation values of NIPP readings were higher than those of the MIPP. This behaviour was consistent with the previously observed random response of the NIPP sensors.

The described selectivity data confirmed that the imprinted sites played a crucial role for the molecular recognition process and were clear indicators that the MIPP displayed highly selective features for FPB. In general, the specific molecular recognition established by the imprinted sites depends on two main factors: the molecular dimension and shape of the template, as well as matching degree of the bonding sites [40]. Considering the results obtained, it was clear that FPB could specifically occupy the imprinted binding sites in the interstices of the opal structure of the MIPP film, thereby confirming that good complementary shape, size and interaction sites were being suitably formed.

PLEASE INSERT FIGURE 4 HERE

3.4. Reusability

The ability to reuse a protein sensor is an important quality index for a novel sensor, since it is a key factor to ensure cost-effectiveness. In this study, this feature was investigated by conducting three rebinding/eluting cycles. The MIPP was first equilibrated, then incubated with a 22 ng mL^{-1} FPB solution, and finally regenerated by washing with sulphuric acid to remove the bounded FPB from the imprinted sites. The cycle of incubation and extraction was repeated successively.

In the first two cycles, the maximum peak intensity of the blank signal in the MIPP film was about 9000 (a.u.) and decreased to about 2000 (a.u.) after FPB rebinding. After the second cycle, the sensor started to show irreproducible and unstable readings. The relative standard deviations observed were in average of 9.7%, ranging from 7.3% to 12.1%. A similar experiment was made with the control NIPP and no significant differences in intensity were found.

The blank signal shifted to lower values on the third cycle, but the subsequent FPB incubation shifted the signal to similar values of those in previous cycles, thereby confirming that the equilibrium between bound and unbound FPB in solution was achieved in the same level as before. Thus, the shifted blank signal could indicate (i) that some FPB units from the previous incubation were steadily bound to the imprinted sites or else entrapped within the polymeric network, (ii) or that the polymeric network was damaged by the consecutive acidic washing. Considering that the NIPP signals were also altered by the third cycle, it seemed plausible that the polymeric network was indeed damaged from this point on.

PLEASE INSERT FIGURE 5 HERE

3.5. Real samples analysis

Human urine samples from healthy individual were spiked with known concentrations of FPB, aiming to evaluate the usefulness of the MIPP sensor on a close-to-real condition. The concentration levels selected for this purpose were 30, 100 and 350 ng mL^{-1}, simulating different clinical conditions. These concentration levels were added directly into the human urine and each solution was diluted by 50-fold and analysed in triplicate. The obtained averages and the corresponding RSD values are indicated in table 1.

In general, the average values were consistent with the spiked levels, shifting within -15% to 9% of the theoretical concentration, with RSD values ranging from 12% to 17%. Thus, the analysis of

samples with concentrations ranging from 0.2 to 22.0 ng mL^{-1} produced accurate data, meaning that this interval should be employed under practical scenarios.

Overall, the results obtained herein suggest that the MIPP sensor may lead to accurate and reproducible readings of FPB in human urine of healthy or diseased individuals.

PLEASE INSERT TABLE 1 HERE

4. Conclusions

A MIPP sensor was successfully constructed to detect FPB, a biomarker of VTE, in urine. To the best of our knowledge, this work is the first one using an opal PC merged with molecular imprinting for sensing a protein biomarker in a biological matrix at clinical relevant levels. The straightforward approach of self-assembly silica nanoparticles enabled obtaining an opal film for the label-free detection of FPB. By combining the selectivity of the MIP materials and the organized structure of a PC, the MIPP sensor demonstrated high selectivity and sensitivity for the target molecule, and displayed low detection limits and reusability features.

The low detection limit achieved suggests that the proposed MIPP sensor is a reliable approach to detect VTE biomarkers in urine. Moreover, the linear response range of detection allows using this sensor before the disease, at the onset and at various stages of disease, as well as for treatment monitoring. Therefore, the future perspectives for cost-effective routine sample testing, enabling rapid and non-invasive screening of VTE, are very promising.

Authors contribution

Sara Resende: investigation, methodology, validation, visualization, formal analysis, data curation, and witting - original draft. Manuela Frasco: conceptualization, funding acquisition, supervision, work administration and writing - review & editing. Goreti Sales: supervision, funding acquisition, and writing - review & editing.

Declaration of interests

The authors declare that they have no known competing financial interests or personal relationships that could have appeared to influence the work reported in this paper.

Conflicts of Interest

The authors declare no conflict of interest.

Acknowledgments

The authors gratefully acknowledge the financial support from projects STRIP2SENSE (NORTE-01-0145-FEDER-024358-SAICT-POL/24358/2016) and IBEROS (Instituto de Bioingeniería en Red para el Envejecimiento Saludable, INTERREG POCTEP/0245_IBEROS_1_E) supported by FEDER, also within the cooperation region of Galicia/Spain and North of Portugal, and by national funds from Fundação para a Ciência e a Tecnologia (FCT). Sara Resende thanks FCT for the PhD grant ref. SFRH/BD/139634/2018.

Supplementary Information: Supplementary information associated with this article can be found below.

References

[1] M.G. Beckman, W.C. Hooper, S.E. Critchley, T.L. Ortel, Am J Prev Med, 38(2010) S495-501.
[2] J.A. Heit, Nat Rev Cardiol, 12(2015) 464-74.
[3] J. Khalil, B. Bensaid, H. Elkacemi, M. Afif, Y. Bensaid, T. Kebdani, et al., World J Surg Oncol, 13(2015) 204.
[4] S. Ikushima, R. Ono, K. Fukuda, M. Sakayori, N. Awano, K. Kondo, Jpn J Clin Oncol, 46(2016) 204-8.
[5] A.A. Khorana, M. Carrier, D.A. Garcia, A.Y. Lee, J Thromb Thrombolysis, 41(2016) 81-91.
[6] C.I. Coleman, A.G.G. Turpie, T.J. Bunz, J. Beyer-Westendorf, J Thromb Thrombolysis, (2018).
[7] G. Lippi, G. Cervellin, M. Franchini, E.J. Favaloro, J Thromb Thrombolysis, 30(2010) 459-71.
[8] V.C. Rodrigues, M.L. Moraes, J.C. Soares, A.C. Soares, R. Sanfelice, E. Deffune, et al., B Chem Soc Jpn, 91(2018) 891-6.
[9] S. Bostrom, E. Holmgren, O. Jonsson, B. Lindstrom, L. Stigendal, Acta Neurochir, 88(1987) 49-55.
[10] T.A. Morris, J.J. Marsh, C.M. Burrows, P.G. Chiles, R.G. Konopka, C.A. Pedersen, Thrombosis Research, 110(2003) 159-65.
[11] Q. Zhang, M.J. Serpe, S.M. Mugo, Polymers-Basel, 9(2017).
[12] R.V. Nair, R. Vijaya, Progress in Quantum Electronics, 34(2010) 89-134.
[13] Y.-n. Zhang, Y. Zhao, R.-q. Lv, Sensors and Actuators A: Physical, 233(2015) 374-89.
[14] C. Fenzl, T. Hirsch, O.S. Wolfbeis, Angew Chem Int Ed Engl, 53(2014) 3318-35.
[15] W. Chen, Z. Meng, M. Xue, J. Shea Kenneth, Mol Impr2016, pp. 1-12.
[16] Q. Yang, H.L. Peng, J.H. Li, Y.B. Li, H. Xiong, L.X. Chen, New J Chem, 41(2017) 10174-80.

[17] A.J. Kadhem, S.T. Xiang, S. Nagel, C.H. Lin, M.F. de Cortalezzi, Polymers-Basel, 10(2018).
[18] Y.A. Zhang, S.M. Huang, C.T. Qian, Q.Z. Wu, J.F. He, J Appl Polym Sci, 133(2016).
[19] N. Sai, Y. Wu, G. Yu, Z. Sun, G. Huang, Talanta, 161(2016) 1-7.
[20] Z.K. Yang, D.J. Shi, M.Q. Chen, S.R. Liu, Anal Methods-Uk, 7(2015) 8352-9.
[21] L. Meng, P.J. Meng, Q.Q. Zhang, Y.J. Wang, Chinese J Anal Chem, 43(2015) 490-6.
[22] F. Xue, Z.H. Meng, Y.F. Wang, S.Y. Huang, Q.H. Wang, W. Lu, et al., Anal Methods-Uk, 6(2014) 831-7.
[23] H.L. Peng, S.Q. Wang, Z. Zhang, H. Xiong, J.H. Li, L.X. Chen, et al., J Agr Food Chem, 60(2012) 1921-8.
[24] C. Guo, C.H. Zhou, N. Sai, B.A. Ning, M. Liu, H.S. Chen, et al., Sensor Actuat B-Chem, 166(2012) 17-23.
[25] Z. Wu, C.A. Tao, C.X. Lin, D.Z. Shen, G.T. Li, Chem-Eur J, 14(2008) 11358-68.
[26] X.B. Hu, G.T. Li, J. Huang, D. Zhang, Y. Qiu, Adv Mater, 19(2007) 4327-+.
[27] Y.J. Zhao, X.W. Zhao, J. Hu, J. Li, W.Y. Xu, Z.Z. Gu, Angew Chem Int Ed Engl, 48(2009) 7350-2.
[28] W. Chen, M. Xue, K.J. Shea, Z. Meng, Z. Yan, Z. Wang, et al., J Biophotonics, 8(2015) 838-45.
[29] T. Brooks, C.W. Keevil, Lett Appl Microbiol, 24(1997) 203-6.
[30] W. Stober, A. Fink, E. Bohn, J Colloid Interf Sci, 26(1968) 62-9.
[31] R. P. Buck, E Lindner. Recommendations For Nomenclature of Ion-Selective Electrodes. Pure &App, Chem., 1994, 66, 12, 2527-2536
[32] S.L. Greasley, S.J. Page, S. Sirovica, S. Chen, R.A. Martin, A. Riveiro, et al., J Colloid Interf Sci, 469(2016) 213-23.
[33] T. Wang, L. Xu, Y. Yan, J. Fu, L. Xiuyang, Controllable Synthesis of SiO2 Nanoparticles: Effect of Ammonia and Tetraethyl Orthosilicate Concentration2016.
[34] I. Venditti, I. Fratoddi, C. Palazzesi, P. Prosposito, M. Casalboni, C. Cametti, et al., J Colloid Interface Sci, 348(2010) 424-30.
[35] Y.J. Lee, S.A. Pruzinsky, P.V. Braun, Langmuir, 20(2004) 3096-106.
[36] T. Endo, S. Ozawa, N. Okuda, Y. Yanagida, S. Tanaka, T. Hatsuzawa, Sensor Actuat B-Chem, 148(2010) 269-76.
[37] H. Su, X.R. Cheng, T. Endo, K. Kerman, Biosens Bioelectron, 103(2018) 158-62.
[38] M. Sivakumaran, N. Malton, Blood, 102(2003) 4618-9.
[39] K. Trofatter, M. O. Trofatter, M. R. Caudle, D. Q. Offutt, Detection of Fibrin D-Dimer in Plasma and Urine of Pregnant Women Using Dimertest Latex Assay1993.
[40] X. Wang, Z. Mu, R. Liu, Y. Pu, L. Yin, Food Chemistry, 141(2013) 3947-53.

Sara Resende received a bachelor's degree in Biochemistry and a master's degree in Forensic Chemistry, both from Faculty of Science and Technology of Coimbra University. She worked in a Pharmaceutical Company (Sanofi) and currently is doing a PhD in Biomedical Engineering at Instituto Superior Técnico and the School of Engineering of te Polytechnic Institute of Porto. Her research is focused on molecular imprinted polymers for a photonic sensor to monitor inflammatory bowel disease's.

Manuela Frasco received a degree in Biochemistry in 2000 and a PhD in Biomedical Sciences in 2007, both from the University of Porto. She is currently a postdoctoral researcher of the research group BioMark, Sensor Research at the School of Engineering, Polytechnic Institute of Porto. Her

research interests are mainly focused on nanomaterials-based sensors, biopolymers, biomimetic sensing and bioinspired photonics.

Goreti Sales received a degree in pharmaceutical sciences in 1994 and a PhD in analytical chemistry in 2000, all from the Faculty of Pharmacy of Porto University. She is adjunct professor in the Polytechnique Institute, School of Engineering, since 2006. Her research interests are mainly devoted to research on biomimetic nanomaterials and biosensing devices. She is the founder of the research group BioMark, Sensor Research (in 2011) and she was awarded (in 2012) a Starting Grant by the European Research Council, targeting a new technical approach that merges biosensors with solar cells. She is currently coordinating the FET-Open project (H2020) MindGAP.

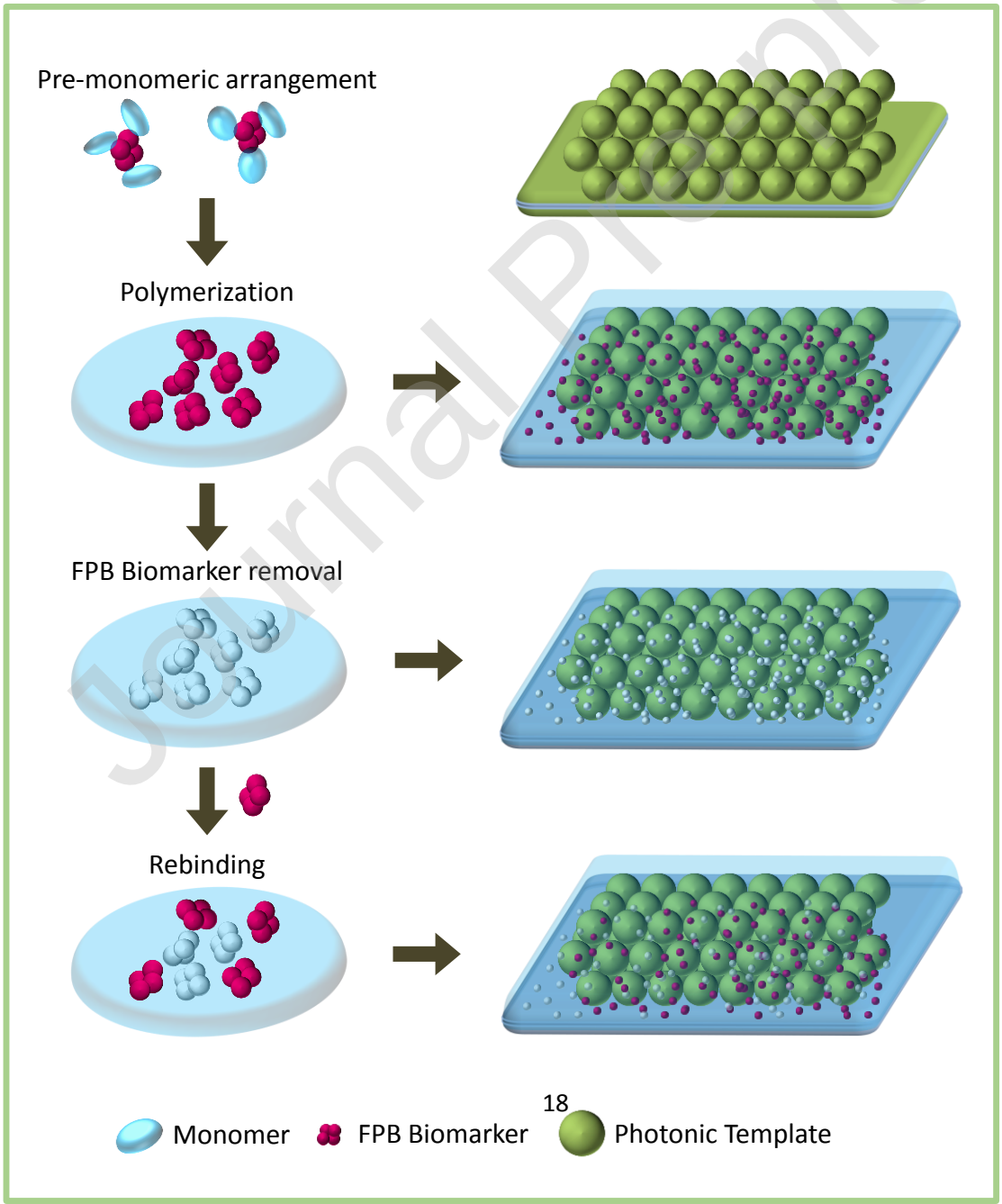

Fig. 1. Schematic illustration of the procedure used to prepare the MIPP film: in the polymerization step, a pre-polymer solution is infiltrated on silica photonic crystal array previously assembled on a glass substrate, followed by template removal to obtain the polymer nanocavities with specificity for FPB.

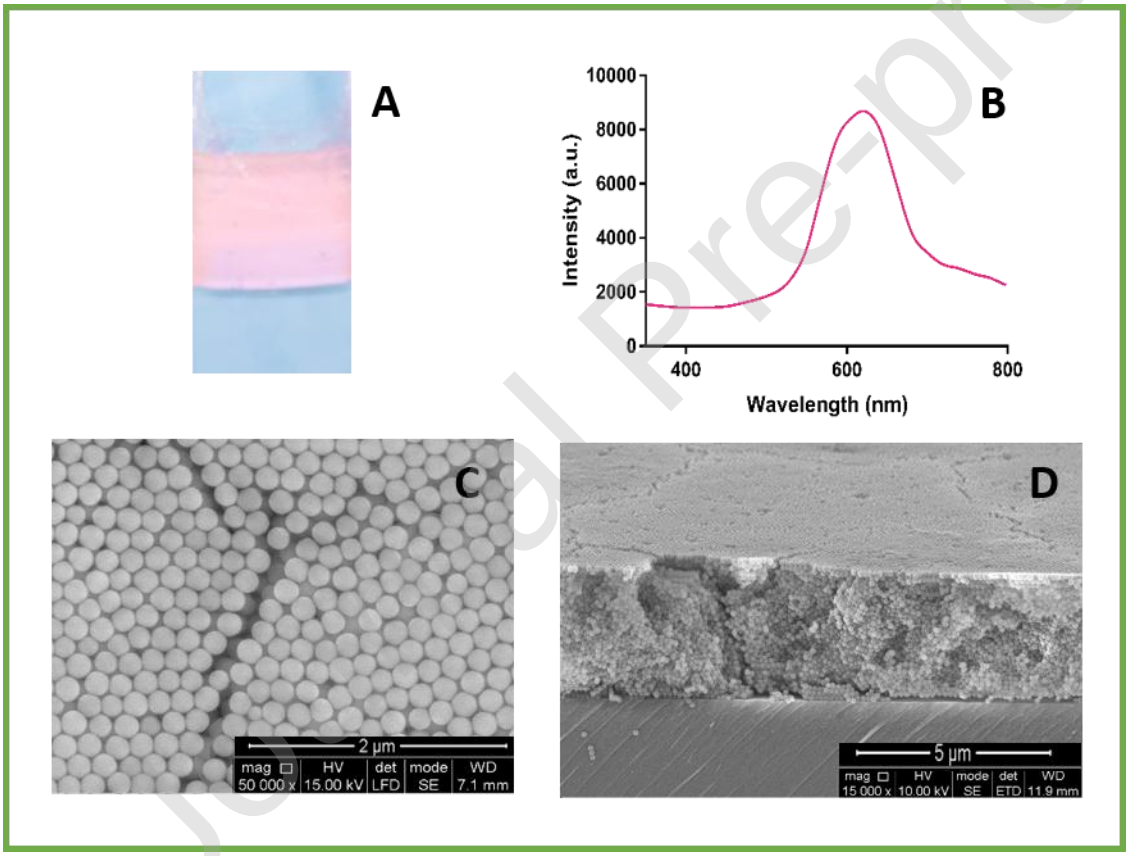

Fig. 2. Picture of an opal film of silica nanoparticles with diameter of 270 ± 10 nm (A), the corresponding reflectance spectra (B), and the close-packed crystal structure as observed in SEM images of the top layer (C) and cross-section (D).

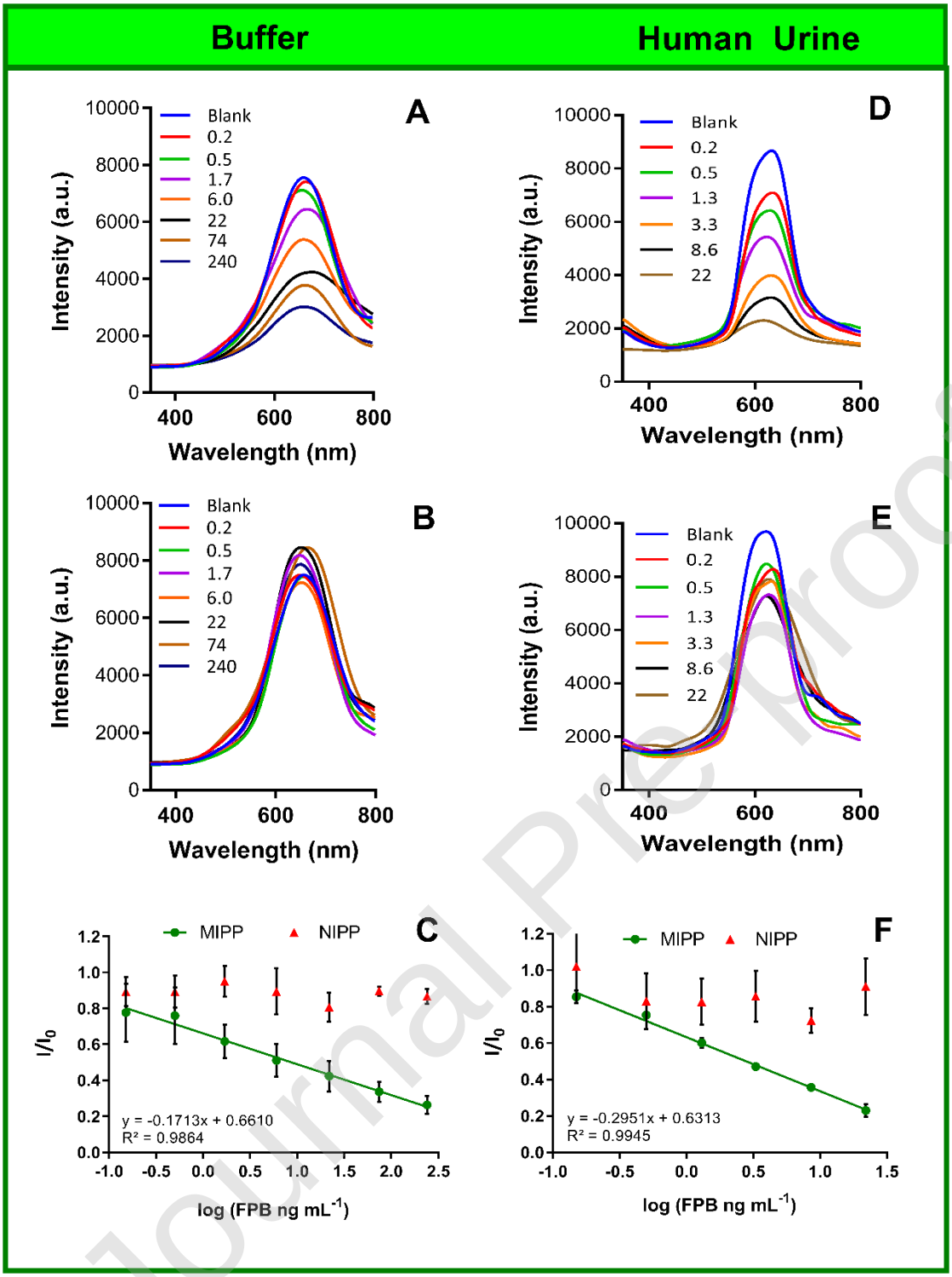

Fig. 3. Optical response of MIPP (A, D) and NIPP (B, E) to FPB obtained in MES buffer (A, B, in 0.1 mol L^{-1}, pH 6) or in human urine (D, E, in 50-fold diluted), expressed by reflectance intensity for several FPB standard in ng mL^{-1}, with the corresponding calibration curves (C, in buffer; F, in human urine) (n = 3).

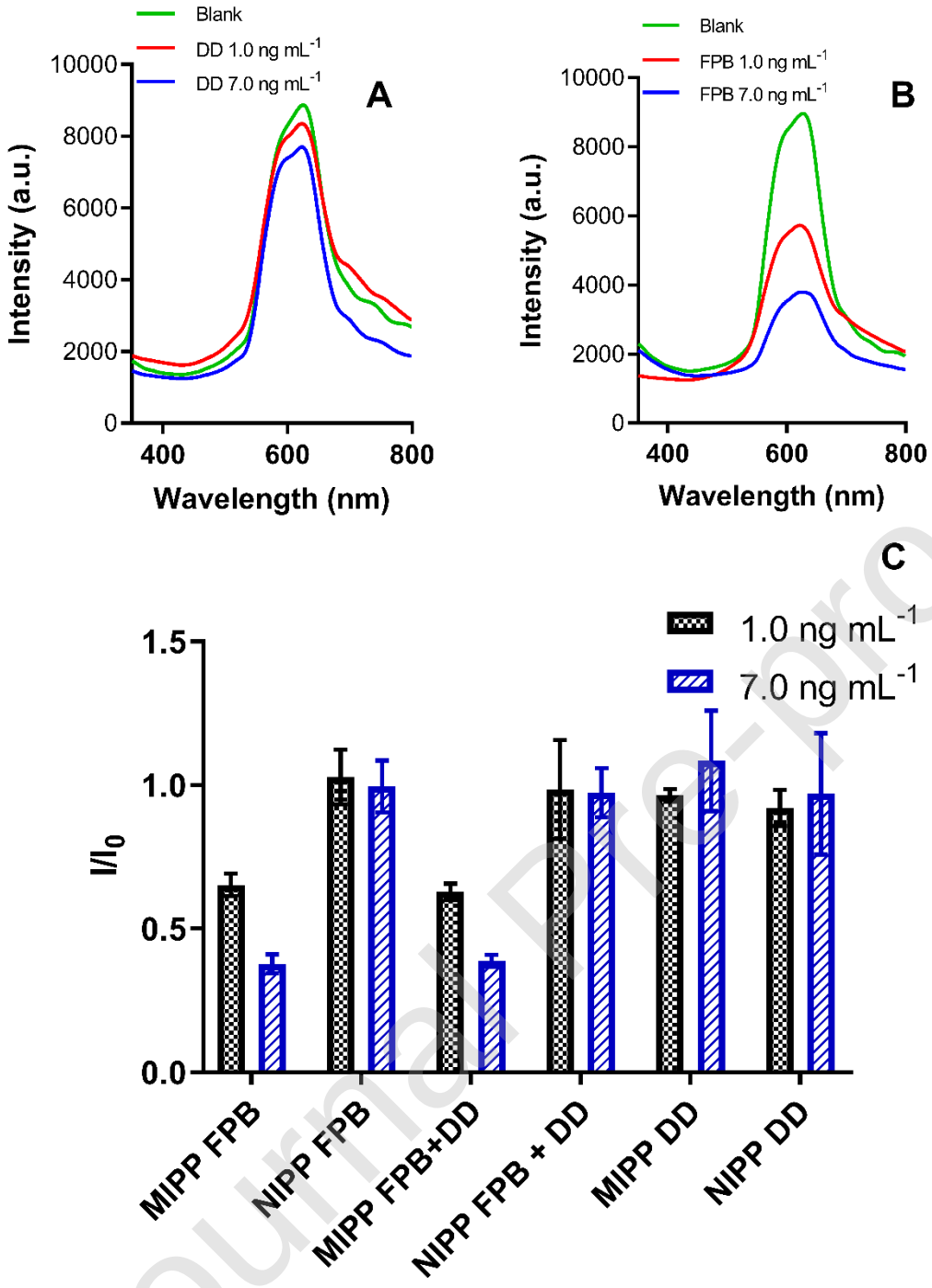

Fig. 4. Representative reflectance spectra of MIPP sensor to single solutions of DD (A) and FPB (B) and to mixed solutions of both peptides (C) at two different final concentrations, 1.0 ng mL^{-1} and 7.0 ng mL^{-1}, prepared in human urine (diluted 50-fold) (n=3). The relative response of MIPP and NIPP is also shown (C) (n = 3).

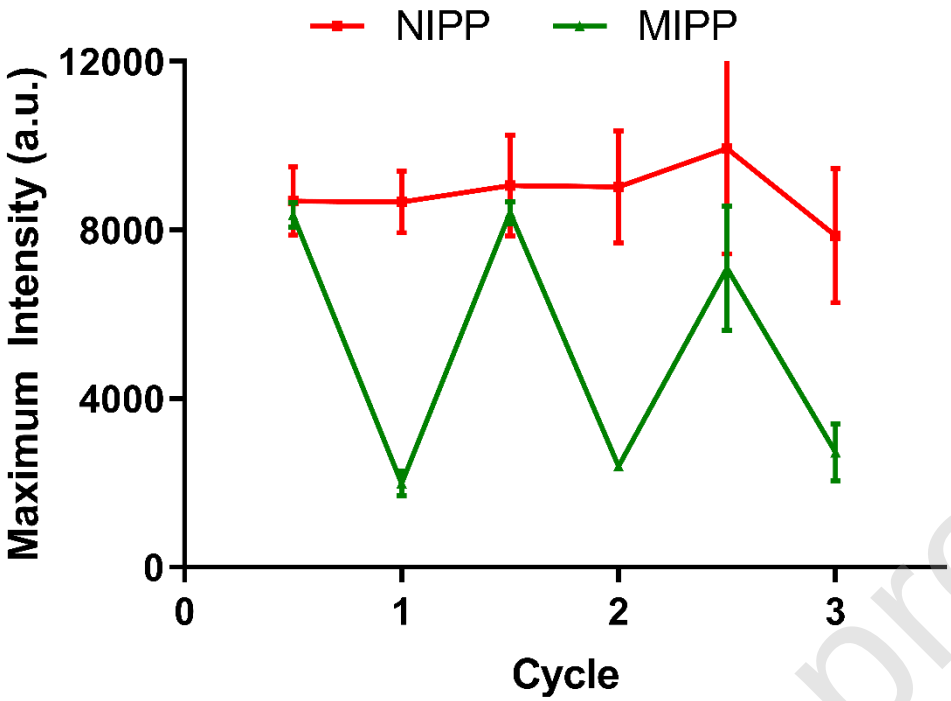

Fig. 5. Representative signal change of the MIPP sensor upon several cycles of incubation in 22 ng mL^{-1} of FPB and regeneration in acidic solution, along with the response of the NIPP sensor under the same conditions.

Table 1. The theoretical concentrations of spiked human urine samples and the corresponding experimental concentrations provided by the MIPP sensor, along with the bias and the RSD (n = 3).

Theoretical concentration (ng mL^{-1})	Experimental concentration (ng mL^{-1})	Bias (%)	RSD (%)
30	27	-8	13
100	109	9	12
350	298	-15	17